Thermal Investigation of an Infrared Reflow Oven with a Convection Fan

Mi Ro Kim*, Young Ki Choi, Gyu Bong Lee***, Il Yong Chung***, Jung Duck Kim**** and Jung Hee Lee****

(*Received October 4, 1997*)

A two-dimensional numerical model for an infrared reflow soldering with a convection fan is used by modifying the Eftychiou's numerical modeling. The two-dimensional tunnel model which predicts convective conditions within the reflow oven are solved using the finite volume method with the SIMPLER algorithm. The card model solves the transient two-dimensional heat conduction equation in conjunction with a radiative heat transfer analysis. We also performed an experiment to validate the numerical modeling. The numerical result shows excellent agreement with experimental data. Based on the capability of this model, parametric simulations are performed to determine the thermal response of the solder to variations in the oven operating conditions and heat transfer conditions. This study shows that radiation and conveyor velocity are important factors in the preheat region.

Key Words: Infrared Reflow Oven, Convection Fan, Card Model, Tunnel Model, Soldering, Finite Volume Method

Nomenclature

A : Area
h : Convective heat transfer coefficient
k : Thermal conductivity
T : Temperature
q'' : Energy per unit area
u, v : x and y velocity components
Γ : Diffusion coefficient
ρ : Density
ϕ : General variable

1. Introduction

In recent years, reliable soldering methods have become a big issue in the area of surface mount technology (SMT). Reflow soldering methods such as infrared heating, vapor phase soldering and infrared heating with a convection fan are used in high density surface mount technology. Infrared reflow soldering with a series of panel heaters is a common technique used in the printed circuit assembly due to its instantaneous heating. Several types of infrared reflow soldering have been proposed and tested. Infrared reflow soldering with a convection fan can cover the weakness of local excessive heating of the infrared heater with hot air flow by the convection fan. To design the reflow soldering equipment and its operating conditions, the heat transfer mechanism in the reflow oven has to be identified and the thermal response of the card assembly has to be obtained for the oven operating conditions.

Lichtenberg and Brown(1987) performed an experimental study to determine the components thermal response to variations in oven operating conditions and heat transfer conditions. Fernandes et al. (1992) measured the thermal response for a simulated card assembly and proposed a simple numerical model to identify and quantify the heat transfer mechanism. Eftychiou et al.

* Automotive Technology, Daewoo I. A. E., Yongin, Kyunggi-Do, 449-800, KOREA
** Dept. of Mech. Eng., Chung-Ang Univ., Seoul, 156-756, KOREA
*** KAITECH, ChonAn, ChungNam,, KOREA
**** Samsung Aerospace Industries Ltd. Kiheung Kyunggi-Do, KOREA

(1992) proposed a numerical model to divide the reflow furnace into a tunnel model and a card model. They assumed the air flow was fully developed and laminar in the tunnel model and used these conditions, along with radiative heat transfer analysis and a two-dimensional conduction analysis, to predict the thermal response of a card assembly as its components are soldered. Also they solved a simplified 2-D model which accounted for coupled radiation, mixed convection and conduction analysis using the finite volume method (Eftychiou et al., 1993).

In this paper, a two-dimensional numerical model for the infrared reflow soldering with a convection fan is developed by modifying the Eftychiou numerical modeling(Eftychiou et al., 1992). To reduce the computational expense, the heat transfer mechanism is separated into large (tunnel) and small(card) scale processes. The tunnel model predicts the two-dimensional convective condition within the reflow oven using the finite volume method with the SIMPLER algorithm(Patankar, 1980). The card model solves the transient two dimensional heat conduction equation in conjunction with a radiative heat transfer analysis. We also perform the experiments to validate the numerical modeling.

2. Governing Equations

2.1 Governing equations of the tunnel model

Eftychiou et al. (1992) assumed the air flow was fully developed laminar flow in the tunnel model and local convection coefficients were obtained from an empirical correlation. In our case with the convection fan, this fully developed assumption is not appropriate. In our numerical modeling for the tunnel model, a set of elliptic partial differential equations governing mass, momentum, energy conservation for the two dimensional laminar unsteady Navier-Stokes equations are solved to get the velocity and temperature profiles.

The general differential equation can be written as follows(Patankar, 1980).

$$\frac{\partial}{\partial t}(\rho\phi)+\frac{\partial J_x}{\partial x}+\frac{\partial J_y}{\partial y}=S \tag{1}$$

where J_x, J_y are the total(convection plus diffusion) fluxes defined by

$$J_x \equiv \rho u\phi - \Gamma\frac{\partial\phi}{\partial x} \text{ and } J_y \equiv \rho v\phi - \Gamma\frac{\partial\phi}{\partial y} \tag{2}$$

2.2 The governing equations of the card model

The heat diffusion equation is applied to the card model

$$\frac{\partial T}{\partial t}=\frac{\partial}{\partial x}\left(\alpha\frac{\partial T}{\partial x}\right)+\frac{\partial}{\partial y}\left(\alpha\frac{\partial T}{\partial y}\right)+S \tag{3}$$

where the source term includes the radiative exchange, the convective heating from the tunnel model and the energy associated with the phase change.

3. Numerical Method

3.1 Grid system

Figure 1 shows the schematics of the infrared reflow oven with the convection fan considered.

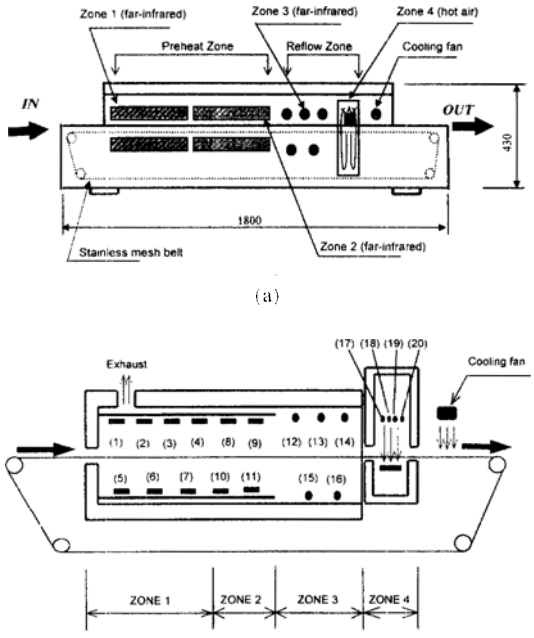

Fig. 1 (a) Schematics of the infrared reflow oven (b) Position of each heater and fan inside the oven.

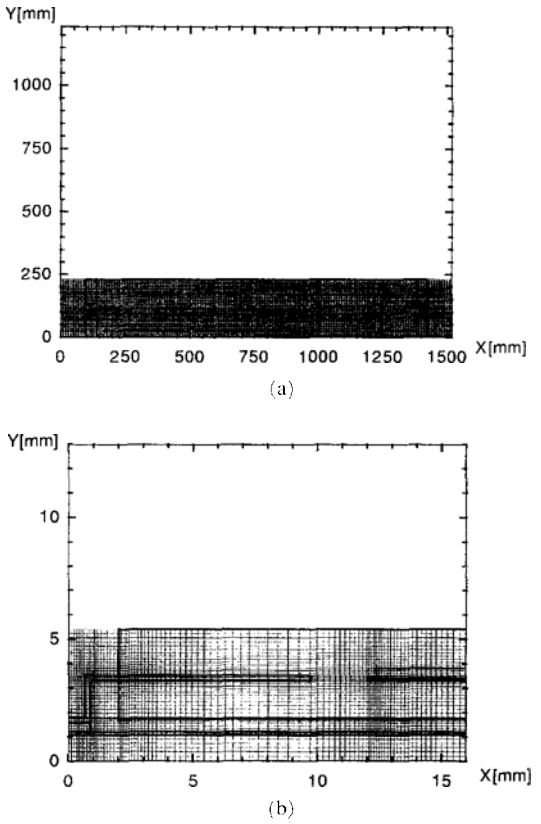

Fig. 2 (a) Grid system of the tunnel model and (b) grid system of the card model.

Due to its simple geometry, the Cartesian coordinate system is used and the variables are arranged as staggered. We performed the calculation using three different grid systems such as 72×24, 143×48 and 286×96 grids to check the grid dependency. The calculated results showed grid independency for over 143×48 grids. Figure 2 shows the 143×48 grid system used for the tunnel model and the 91×44 grid system for the card model. Grids are concentrated near the solder and the die pad.

3.2 Numerical analysis

Algebraic equations are obtained by the finite volume approach. The power-law scheme (Patankar, 1980) for the convection and the central difference scheme for the diffusion are used.

To solve the discretized equation, TDMA algorithm is used in conjunction with a line-by-line method. To speed up the numerical convergence, the SIMPLER algorithm (Patankar, 1980) is applied to solve the pressure and the momentum equations. The simulations were performed on a SUN axil 311 workstation and required 30 hours to (0.1s time step) the card model and 40 hours to the two-dimensional tunnel model.

3.2.1 The tunnel model

The hot air circulation fan at zone 4 (see Figure 1) is treated as a momentum source. The heater at zone 4 is also treated as a heat source. We neglect thermal stratification because mean air velocity is very small. Volumetric radiative absorption, emission and scattering within the air are also negligible. Properties of air such as k, c, μ and ρ are treated as functions of temperature.

3.2.2 The card model

The card model needs a convective condition, which is obtained from the tunnel model and radiative heat transfer energy. First of all, we calculate the view factor by using the Hottel's Crossed-String Method (Siegel, 1981). Then the radiative heat transfer energy is found from the diffuse gray radiation enclosure analysis (Incropera, 1990). Reradiation from the card is neglected because the length of the card is extremely short compared with the length of the tunnel.

3.3 Boundary conditions

In the tunnel model, velocity conditions are given from the mass balance. At the wall, no-slip conditions are applied.

The temperature condition of the panel is given by measurements. The symmetry condition is applied between each panel heater.

In the card model, the temperature boundary condition is applied as

$$\text{at } x=0,\ l:\ \frac{\partial T}{\partial x}=0 \tag{4}$$

$$\text{elsewhere}:\ k\frac{\partial T}{\partial y}=q''_{rad}+q''_{conv} \tag{5}$$

$$\text{where, } q''_{conv}=h(T_{tunnel}(t)-T(x,\ y,\ t)) \tag{6}$$

and the solders solid-liquid phase change is considered from the following equation.

$$\rho_{sol} h_{f,sol} V_{sol} = k_{sol} A_{sol} \frac{\partial T}{\partial n} \Delta t \quad (7)$$

4. Results and Discussion

We analyze a far-infrared reflow system named RF-447. The size and weight of this machine are (W) 1800mm × (D) 680mm × (H) 430mm and 160kg, respectively. It can solder more than 1500 PCB's, sized 100mm × 200mm, per day. Figure 1 shows the schematics in the infrared reflow oven. The size of the heating zone is (W) 300mm × (L) 1200mm. Size of the card is 28mm × 28mm × 6mm and velocity of the conveyor is 6mm/s. Heater in the preheat zone is constructed by far-infrared ceramic plates and the heater in the reflow zone is constructed by far-infrared ceramic rod heater. The soldering region (zone 4) is heated by the hot air circulation using the forced convection fan. Each heater can be controlled by the external temperature controller. Table 1 indicates the experimental temperature conditions.

Table 1 Control condition of the tunnel model.

Temperature of each heater			
1 : 369℃	6 : 302℃	11 : 195℃	16 : 254℃
2 : 416℃	7 : 357℃	12 : 275℃	17 : 575℃
3 : 389℃	8 : 238℃	13 : 274℃	18 : 589℃
4 : 382℃	9 : 218℃	14 : 276℃	19 : 485℃
5 : 268℃	10 : 224℃	15 : 262℃	20 : 479℃
Temperature of outer controller			
Region 1	Region 2	Region 3	Region 4
225℃	195℃	180℃	245℃
Velocity of fan (Zone 4)			
1.25m/s			

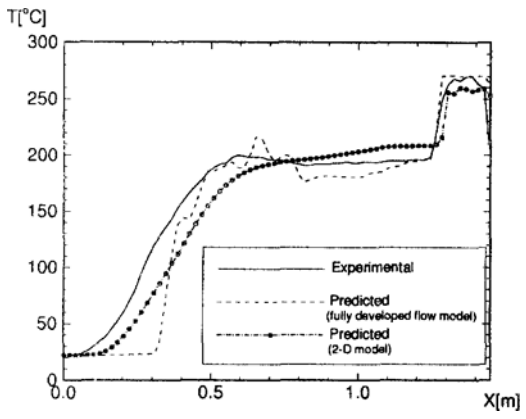

Fig. 3 Numerical results of the centerline air temperature profile compare with the experimental result.

4.1 Result of the tunnel model

Figure 3 shows numerical results of the centerline air temperature profile compared with the experimental data. This comparison shows better agreement between our two dimensional approach and the experimental data than the fully developed air flow approach. Overall temperature profile shows excellent agreement except in the inlet region.

Figures 4 and 5 illustrate the air temperature distribution and the air velocity profile inside the

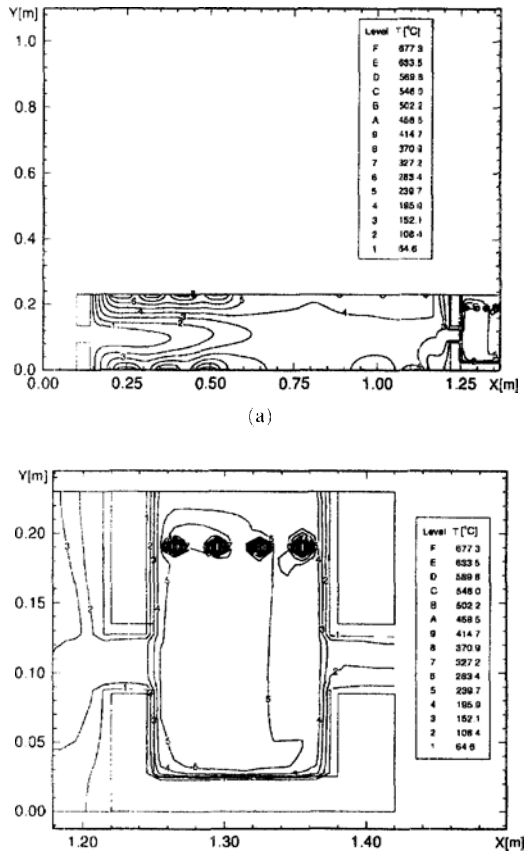

Fig. 4 Air temperature profile inside the tunnel (a) the whole region (b) the soldering zone.

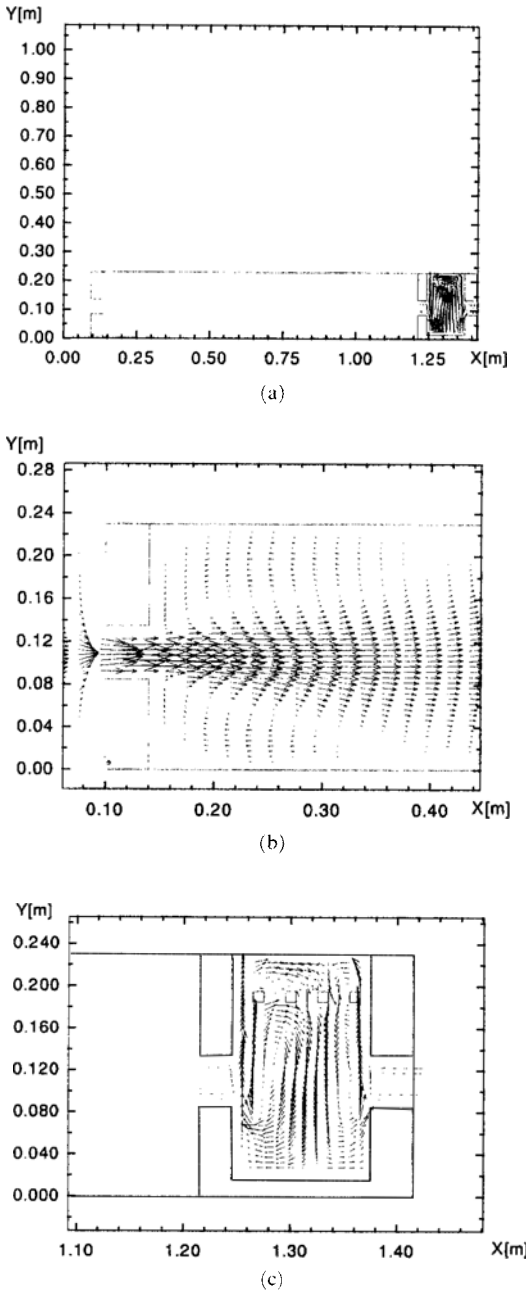

Fig. 5 Air velocity profile inside the tunnel (a) the whole region (b) inlet region (c) the soldering zone.

tunnel, respectively. The air is introduced to the inlet by the convection fan; with a minimal velocity. Therefore the radiative heat transfer is dominant in this region. As the chip goes further, the temperature becomes uniform inside the tunnel.

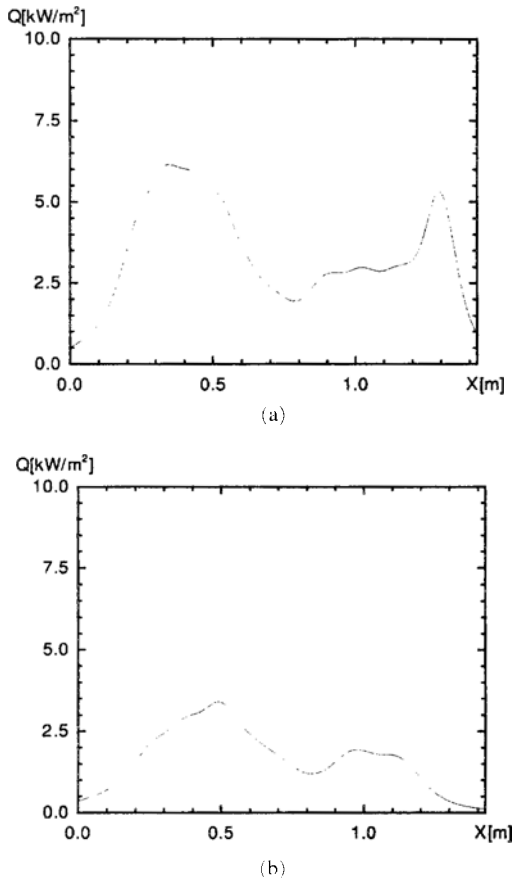

Fig. 6 Radiative transfer to the card assembly (a) top (b) bottom.

Finally the temperature reaches over the melting point at the soldering zone by radiation and convection. The convection fan can improve the quality of the soldering by uniform heating.

4.2 Result of the card model

The radiative heat fluxes, obtained from the diffuse gray radiation enclosure analysis, at the top and bottom of the card are shown in Figure 6. They show the highest heat flux at $x=0.5$m at the bottom. That result compared with the experimental result is also shown in Fig. 7. This result shows excellent agreement with the experimental data. Figure 8 shows the predicted thermal response of the solder compared with the air temperature of the tunnel as the card assembly undergoes. In the entrance region, air and solder temperatures show no difference. The radiative

heat transfer is the dominant factor in this region. As the card goes further, the air temperature becomes higher than the card temperature and the energy is transferred by convection. At middle section heated by the ceramic rod heater, the air temperature becomes uniform and the solder temperature is adjusted. At the soldering zone, the solder temperature reaches over the melting point mainly by convection. Although we consider phase change effect as a source term, its influence is minimal. Figure 9 shows the temperature history inside the card assembly as the card assembly passes the preheat region.

Parametric study is performed to determine the sensitivity of the components thermal response to radiative or convective heat transfer conditions

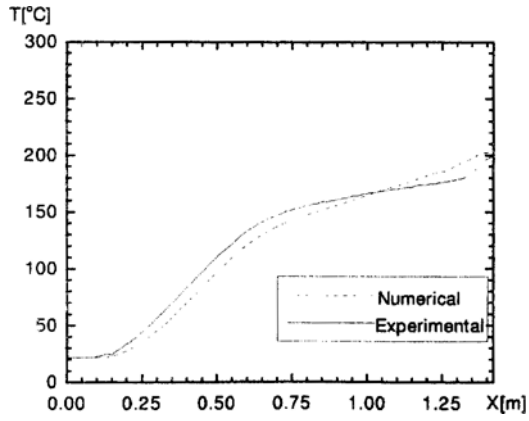

Fig. 7 Solder temperature profile compared with the experimental results.

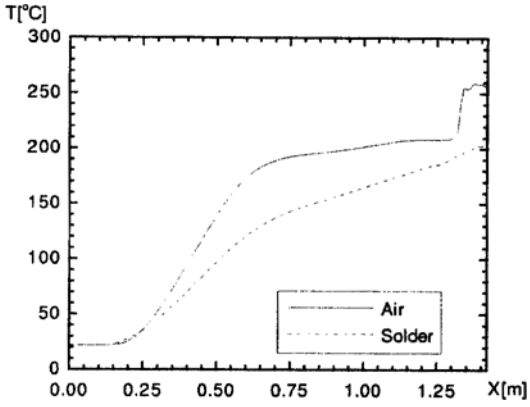

Fig. 8 Solder temperature profile compared with the air temperature profile by the tunnel model.

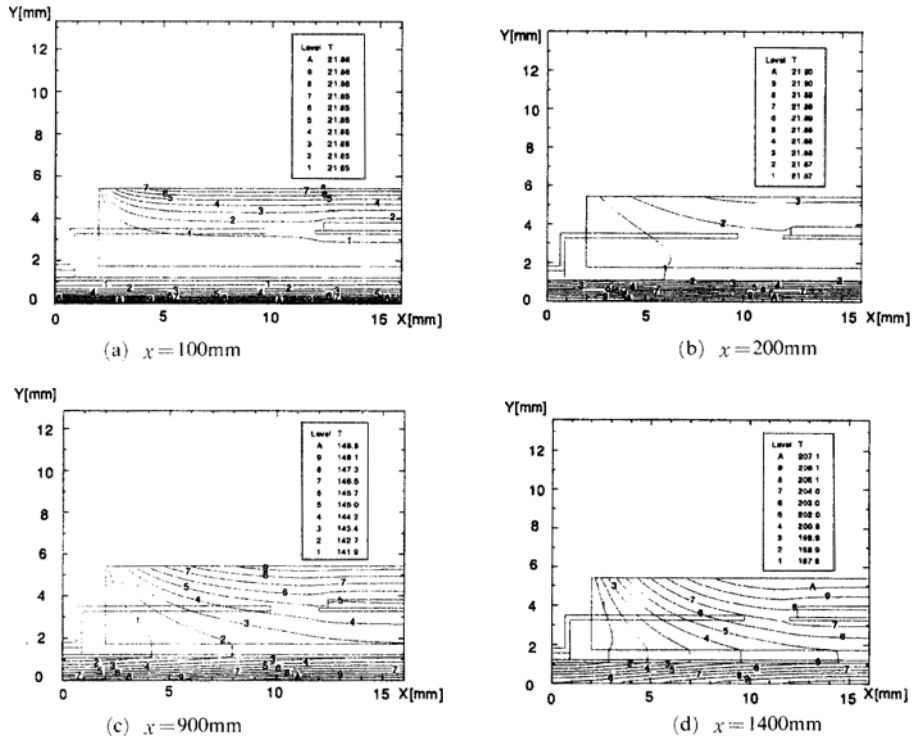

Fig. 9 Temperature distribution inside the card assembly.

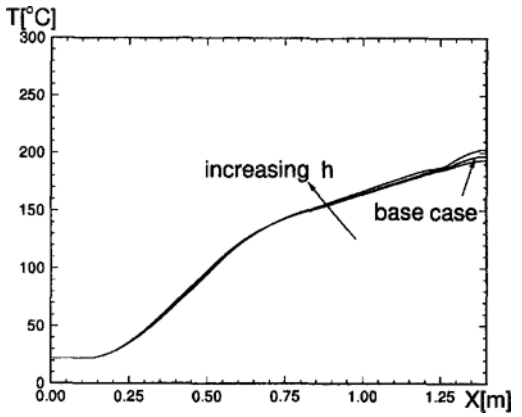

Fig. 10 Sensitivity of the solder temperature to variations in convective coefficients (doubled base case values and half of the base values).

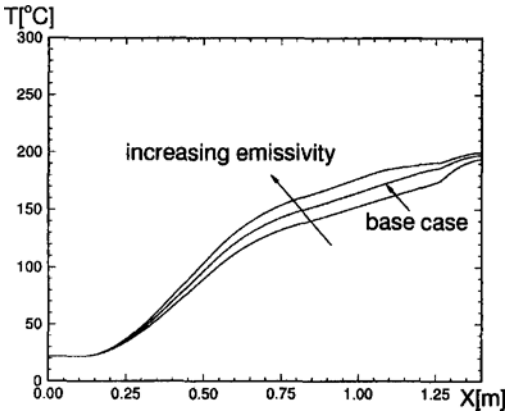

Fig. 11 Sensitivity of the solder temperature to variations in emissivity (1, 0.95 and 0.85).

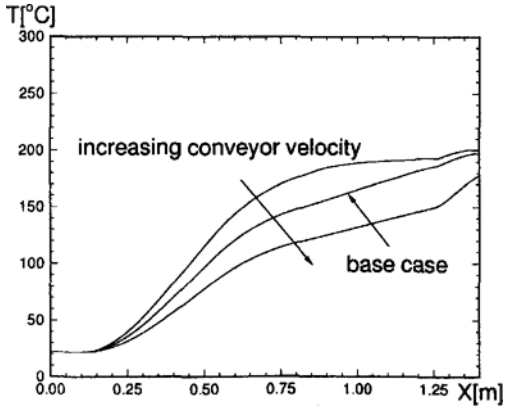

Fig. 12 Sensitivity of the solder temperature to variations in conveyor velocity (4, 6 and 8 mm/s).

and conveyor velocity.

Figure 10 shows the influence of the convective heat transfer coefficient. Although the baseline predictions are compared to those using doubled value and half of the baseline value, it shows no difference except in the soldering zone. The solder temperatures for three different emissivity, $\varepsilon=1$, 0.95, 0.85 respectively, are shown in Figure 11. This figure shows that the radiation is an important factor in the preheat region. Figure 12 shows the sensitivity of the solder temperature due to the conveyor velocity. The different solder temperature histories in Figure 12 occur primarily because of the decrease in heating time associated with increased conveyor velocity.

5. Conclusion

A two dimensional numerical model is used to simulate the infrared reflow soldering with a convection fan and is compared with experimental results. The numerical results on the air temperature inside the tunnel show a good agreement with the experimental data except for the inlet region. The solder temperature profile also shows a good agreement with experimental data. Therefore this model can be used to find the optimal design condition for the infrared reflow soldering oven. From the parametric study, the influence of convection and radiation is identified. It is also found that the air velocity is an important factor on the solder temperature.

Acknowledgments

This research was sponsored by G7 project, Insertion and Surface Mounting Technology, and partially supported by Turbo and Power Machinery Research Center.

References

Eftychiou, M., Bergman, T. and Masada, G., 1992, Thermal Effects during Infrared Solder Reflow Part II : Heat Transfer Mechanisms, *ASME J. of Electronic Packaging*, Vol. 114, pp. 48～54, March.

Eftychiou, M., Bergman, T. and Masada, G., 1993, A detailed Thermal Model of the Infrared Solder Reflow Soldering, *ASME J. of Electronic Packaging,* Vol 115, pp. 55~62, March.

Fernandes, N. J., Bergman, T. and Masada, G., 1992, Thermal Effects during Infrared Solder Reflow Part I : Heat Transfer Mechanisms, *ASME J. of Electronic Packaging,* Vol. 114, pp. 41~47, March.

Incropera, F. P. and Dewitt, D. P., 1990, *Fundamental of Heat and Mass Transfer,* New York, Wiely and Sons.

Lichtenberg, L. R. and Brown, L. L., 1987, Component Thermal Management in Infrared Solder Reflow, *Int. J. of Hybrid Microelectronics,* Vol. 10, No. 2, pp. 19~26.

Patankar, S. V., 1980, *Numerical Heat and Fluid Flow,* New York, McGraw-Hill.

Siegel, R. and Howell, J. R., 1981, *Thermal Radiation Heat Transfer,* Washington, Hemisphere Publishing Corporation.